



Published in final edited form as:

Ann N Y Acad Sci. 2016 May ; 1371(1): 55–67. doi:10.1111/nyas.12990.

Vision loss in juvenile neuronal ceroid lipofuscinosis (CLN3 disease)

Madhu M. Ouseph^{1,a}, Mark E. Kleinman², and Qing Jun Wang^{1,3,4}

¹Department of Molecular and Cellular Biochemistry, University of Kentucky, Lexington, Kentucky

²Department of Ophthalmology and Visual Sciences, University of Kentucky, Lexington, Kentucky

³Department of Toxicology and Cancer Biology, University of Kentucky, Lexington, Kentucky

⁴Markey Cancer Center, University of Kentucky, Lexington, Kentucky

Abstract

Juvenile neuronal ceroid lipofuscinosis (JNCL; also known as CLN3 disease) is a devastating neurodegenerative lysosomal storage disorder and the most common form of Batten disease. Progressive visual and neurological symptoms lead to mortality in patients by the third decade. Although ceroid-lipofuscinosis, neuronal 3 (*CLN3*) has been identified as the sole disease gene, the biochemical and cellular basis of JNCL and the functions of *CLN3* are yet to be fully understood. As severe ocular pathologies manifest early in disease progression, the retina is an ideal tissue to study in the efforts to unravel disease etiology and design therapeutics. There are significant discrepancies in the ocular phenotypes between human JNCL and existing murine models, impeding investigations on the sequence of events occurring during the progression of vision impairment. This review focuses on current understanding of vision loss in JNCL and discusses future research directions toward molecular dissection of the pathogenesis of the disease and associated vision problems in order to ultimately improve the quality of patient life and cure the disease.

Keywords

Juvenile neuronal ceroid lipofuscinosis; CLN3; vision loss; ocular pathologies; retina

Introduction

Juvenile neuronal ceroid lipofuscinosis (JNCL; originally known as Spielmeier–Vogt–Sjögren–Batten disease or Batten disease, and currently known as CLN3 disease) is a rare autosomal recessive, neurodegenerative lysosomal storage disorder that manifests in early childhood. Symptoms of JNCL (including personality changes, learning impairment,

Address for correspondence: Qing Jun Wang, Department of Molecular and Cellular Biochemistry, University of Kentucky College of Medicine, B163 BBSRB, 741 South Limestone, Lexington, KY 40536. qingjun.wang@uky.edu.

^aCurrent affiliation: Department of Pathology and Laboratory Medicine, Rhode Island Hospital and Brown University, Providence, Rhode Island

Conflicts of interest

The authors declare no conflicts of interest.

declining speech and motor skills, seizures, and vision loss) typically first appear between 4 and 8 years of age but in some cases can start as early as 2 years of age.¹ In females, symptoms occur earlier and are usually more severe compared to males.^{2,3} These eventually lead to premature death, usually by the third decade of life.¹ The disease was originally named after Frederick Batten, a British pediatrician who described the disease in 1903.⁴ Use of the term Batten disease has evolved to include the group of neuronal ceroid lipofuscinoses (NCLs), which is further classified as infantile (INCL), late infantile (LINCL), juvenile (JNCL), or adult (ANCL) on the basis of the age at onset of symptoms, as well as the molecular and genetic bases of various forms of Batten disease.^{5,6} The incidence of Batten disease is estimated to be 2 to 4 per 100,000 births in the United States⁷ and as high as 7 per 100,000 births in Scandinavia.⁸ JNCL is the most common form of Batten disease.

Over the past two decades, mutations in multiple genes have been identified in association with NCLs, with mutations in the ceroid-lipofuscinosis, neuronal 3 (*CLN3*) gene being linked to JNCL.^{7,9} *CLN3*, mapped to chromosome 16p12.1, encodes the 438-amino acid protein product CLN3 or Battenin.^{7,9} Exact localizations and functions of CLN3 are not well defined,^{10–12} but a growing body of data offers critical insight into this enigmatic protein. For example, studies using cell culture models support the notion that CLN3 trafficks through endoplasmic reticulum and Golgi to finally reside in endosomal and lysosomal membranes in non-neuronal tissues and is localized to synaptic vesicles, late endosomes, and lysosomes in neuronal tissues.^{13–20} Of more than 60 mutations of *CLN3* that are uncovered in JNCL patients (<http://www.ucl.ac.uk/ncl/CLN3mutationtable.htm>), the most common one is a 966 base-pair deletion (often referred to as 1 kb or 1.02 kb deletion) that leads to skipping of exons 7 and 8 (GenBank accession number: AF077964 or AF077968), with a majority of patients being homozygous for this mutation.^{7,21,22} With advances in next-generation sequencing and as more patients are tested, it is possible that more compound heterozygotes will be discovered.

JNCL is largely considered a neurodegenerative disease as manifested by its clinical and pathological features.²³ Marked pathological changes have been revealed in the brains of JNCL patients using magnetic resonance imaging (MRI), including cerebral and cerebellar atrophy and significant volume reduction in affected areas of the brain.^{24–26} At autopsy, the brains of JNCL patients are smaller, with diffuse loss of neurons and evidence of the characteristic Shaffer–Spielmeyer process in the remaining neurons.²³ In various tissues, JNCL mutations lead to accumulation of autofluorescent lipopigments (i.e., ceroids). In electron microscopic images, these ceroids show characteristic fingerprint profiles that are used as diagnostic criteria for JNCL.^{27–29} Though heterogeneous, the most abundant components of ceroids include the subunit *c* of mitochondrial ATPase F₀ complex,^{30,31} consistent with reduced mitochondrial ATP hydrolysis in skin fibroblasts from JNCL patients.³² Ceroid deposition is also associated with a neurologic autoimmune response, extensive neurodegeneration, and gliosis, which ultimately result in a loss of brain matter and consequential visual and neurological defects.³³

Although the primary focus in JNCL research is on understanding the profound neurological defects, pathologies in non-neuronal cells and organs have also been reported. Nearly half of patients in the late stages of JNCL have cardiac defects with ventricular hypertrophy and

conduction defects, with sinus node dysfunction being the most common.^{34–38} Cardiac evaluation in these patients demonstrates deposition of storage material in the atrioventricular conduction system.³⁷ Characteristic fingerprint profiles have also been reported in patient endothelial cells.^{1,39} This, plus the detection of autoantibodies against central nervous system proteins in patient blood, suggests possible compromise of vasculatures and the blood–brain barrier (BBB).^{40–43} In addition, approximately 30% of circulating lymphocytes in JNCL patients are noted to have cytoplasmic vacuoles.^{44–46}

Ocular pathologies in human patients

Among the early clinical symptoms, functional vision impairment, including loss of visual acuity, nyctalopia, nystagmus, photophobia, and loss of peripheral and color vision, are often the presenting symptoms that lead to referral to an ophthalmologist.⁴⁶ Yet, the sequence of the development of various histopathological features in human eyes is not well described, as the present information is primarily derived from evaluation of eyes from patients in late stages of the disease. Generally, even in advanced cases, the eyes are grossly normal, except for changes in the retina and optic nerve.^{47, 48}

A study of 24 patients showed that the most consistent ophthalmoscopic presentation of JNCL is the diffuse retinal pigment epithelium (RPE) atrophy of the macula, which appeared in 63% of patients.⁴⁷ A “bull’s eye” macular dystrophy (Fig. 1A), which has often been observed anecdotally,^{45,46,49–52} is present in 20% of patients.⁴⁷ Of note, these classic pigmentary macular changes are subtle in early disease stages and can be missed if examination is done without dilation.⁴⁵ Although not routinely used for evaluation of JNCL patients, fluorescein angiography was used in one study to demonstrate marked leakage of dye into the retina in two of five children evaluated, consistent with a potential microvascular defect in JNCL patients.⁴⁵ Moreover, the commonly observed diffuse RPE atrophy of the macula is easily visualized on fluorescein angiography (Fig. 1B) in 93% of patients.⁴⁷ In addition, moderate-to-severe optic disc pallor, attenuated vessels, and thinning of the retinal arterioles that are suggestive of optic nerve and retinal degeneration, were observed in 75% of patients.^{45,47} Only very recently have pathological alterations beyond the retina and the optic nerve (e.g., cataract and secondary glaucoma) been reported to be complications of JNCL.⁵³

A histology study of JNCL eyes showed that the retina is uniformly thinned with severe loss of the photoreceptor, outer nuclear, and outer plexiform layers in the macula and mid-periphery (Fig. 2).⁵⁴ The outer nuclear layer is replaced by villus processes derived from the RPE, as well as hypertrophied Müller cells and macrophages. Scattered and disorganized photoreceptors may be observed in the periphery. In addition, there is atrophy of the nerve fiber layer and ganglion cells coupled with significant gliosis of the optic nerve.^{48,54,55} While Bruch’s membrane is well maintained, the RPE is notably present only in the periphery, with only few RPE cells attached in the macular region, bringing the gliotic layers in direct apposition to Bruch’s membrane. The central residual RPE cells have sparse melanin granules compared to normal cells in the periphery. More conspicuously, the RPE cells in the extramacular region that have migrated along sclerotic retinal vessels lack lipofuscin pigments and are identified only by clumps of melanin granules.⁴⁸ Fluorescent

microscopy demonstrates accumulation of autofluorescent cytoplasmic ceroid granules predominantly in the photoreceptor cell layer,³³ abundantly in retinal ganglion cells, and occasionally in neurons of the inner nuclear layer. The role of the autofluorescent material in the onset and progression of JNCL is unclear. Interestingly, while autofluorescence in the RPE cells of healthy individuals is prominent, autofluorescence in JNCL RPE cells is decreased,^{54,55} which is consistent with photoreceptor cell death and subsequently reduced RPE phagocytosis of outer segments. In the rest of the JNCL eye, autofluorescence is prominent in the epithelial cells of the conjunctiva and ciliary body, but not the cornea. Similar to what is seen in retinitis pigmentosa (RP), JNCL RPE cells are translocated to form bone spicule/corpuscular pigment deposits surrounding retinal blood vessels in the mid-periphery and around the macula.⁵⁴ In electron microscopic images, intracytoplasmic curvilinear inclusions are noted in fibrocytes, pericytes, glial cells, RPE cells, and ganglion cells.³³ The inclusions in ganglion cells contain abundant irregular trilaminar membranes of 8–10 nm thickness, which sometimes are arrayed in curvilinear fashion (Fig. 3A). Some inclusions in ganglion cells show fingerprint profiles (Fig. 3B), although these are relatively rare in neurons as compared to in non-neuronal cells, such as mural cells of small vessels.^{48,54} Though not well characterized, a significant element of inflammation is hypothesized to be associated with JNCL retinal changes, with observations of cell infiltration into the vitreous and of anti-retinal antibody (e.g., anti-carbonic anhydrase II) reactivity.⁵⁶

Besides ocular histopathological features, JNCL patients also show profound electroretinogram (ERG) abnormalities (Fig. 4).^{46,49–52,57} According to the International Society for Clinical Electrophysiology of Vision (ISCEV) standards, full-field ERG recorded with a dim white flash that is below the threshold for eliciting a cone response represents the rod response; the maximal response to intense white light represents a mix of rod- and cone-mediated activities; the cone response can be isolated by eliminating the rod response using either white light flickering at 30 Hz, which exceeds the fusion frequency of rods, or by white light with saturating intensity for rods (e.g., 34 cd/m²) following 10 min light adaptation at 1.5 log cd/m² (i.e., photopic).⁵⁷ Using the ISCEV standards, the ERGs of JNCL patients show significantly reduced rod- and cone-response amplitudes even at early disease stages. At advanced disease stages, the ERGs of JNCL patients show unrecordable rod-mediated activity and significantly reduced cone-mediated activity. In some cases, scotopic b-wave amplitudes may appear to be more severely depressed than a-wave amplitudes, leading to an electronegative ERG and indicating greater impairment in the inner retina than in photoreceptors. Delayed cone b-wave implicit times have also been noted in JNCL, suggesting progressive, rather than stationary, retinal degeneration.^{46,50,51,57} In comparison to typical RP, JNCL patients often show rapid progression of vision impairment, with extensive retinal degeneration and significant loss of the ERG signal in 1–2 years after presentation.^{33,48,57}

Despite the usefulness of ERG in diagnosing JNCL, less invasive and more disease-specific diagnostic approaches for retinal abnormalities of JNCL are desired. Recently, Hansen *et al.* used optical coherence tomography (OCT) to examine two JNCL patients and revealed prominent thinning of outer nuclear and photoreceptor layers, which is consistent with the aforementioned histological findings, as well as abnormally homogenous optical reflectivity

in the inner retinal layers along with the presence of hyperrefractive granules in RPE.⁵⁸ Moreover, using spectral domain OCT and confocal scanning laser ophthalmoscope (cSLO), Dulz *et al.* found that all of the 11 patients tested showed a JNCL-specific striated macular pattern of unknown origin within the papillomacular bundle.⁵⁹ However, determining whether this may provide an early diagnosis specific for JNCL would require more patient data.

Ocular pathologies in mouse models

CLN3 orthologs are expressed in the retina and optic nerve in mouse and non-human primates.^{60,61} While experimental evidence primarily supports CLN3 localization in lysosomal and endosomal membranes, it was shown to be localized to mitochondria in the murine retina using rabbit antiserum against synthetic mouse Cln3 peptide. The signal was most obvious in Müller cells and inner nuclear layer neurons, with a limited presence in photoreceptor cells and sparing the other cell types, including RPE.⁶⁰ Difficulties in studying CLN3, including its subcellular localization, stem from its low expression levels and hydrophobic nature, the latter of which has hindered development of a specific antibody against full length CLN3/Cln3 and leads to dependence on peptide-derived antibodies, yielding varying and conflicting data.^{10–12,60,62}

To circumvent the difficulties in generating specific anti-CLN3 antibodies, a mouse model with β -galactosidase knock-in (replacing part of exon 1 and all of exons 2–8) into the *Cln3* locus was engineered (*Cln3^{LacZ/LacZ}*; generated in 129/Sv embryonic stem (ES) cells and backcrossed to C57BL/6J mice).⁶³ This mouse model shows endogenous expression of Cln3 reporter in different tissues, including the visual cortex (transient presence before P30, primarily in the deep layers such as layer VI and the subplate zone), the dorsal lateral geniculate nucleus (LGNd), and the retina (inner nuclear layer, primarily the bipolar cells, and to a lesser extent, the photoreceptor layer).^{63,64} The Cln3 reporter in the retina is expressed substantially later than in the cerebral cortex, with expression of the inner nuclear layer preceding the outer nuclear layer. This pattern of expression closely correlates with the pattern of visual impairments in the other JNCL mouse models (as discussed below). Surprisingly, the ganglion cells appear to express low levels of Cln3 reporter, in contrast to the extensive ganglion cell pathologies reported in other JNCL mouse models. Of note, possible differences between the intracellular processing of the native Cln3 protein and that of the reporter protein could be a potential caveat in investigating the localization and function of native Cln3. Because β -galactosidase knock-in results in deletion of a large portion of the *Cln3* gene, this mouse model has the potential to be a good JNCL model. *Cln3^{LacZ/LacZ}* mice have been shown *in vivo* to have abnormal BBB physiology in response to hypotonic shock, likely resulting from misregulated microdomain-associated protein trafficking and ARF1-Cdc42-mediated fluid phase endocytosis in brain endothelial cells.^{63,65} However, detailed retinal phenotypes of this JNCL mouse model are yet to be characterized.

Besides the β -galactosidase knock-in *Cln3* reporter mice, there are three well-characterized JNCL mouse models. In the first mouse model, exons 1–6 of *Cln3* were disrupted, creating a null allele (*Cln3^{-/-}*; generated in 129/SvEvTac (129S6) TC1 ES cells).^{66,67} On a 129/

SvEvTac background, there was significant accumulation of intracellular autofluorescent inclusions in the *Cln^{-/-}* brain as well as in the retinal ganglion cells and inner nuclear layer as early as 2.5–3 months old when no obvious visual impairment was observed,^{67, 68} suggesting that this autofluorescent material may not be critical in the progression of the ensuing retinal degeneration. At 15 months old, the fundus autofluorescence pattern was enhanced in the retinal ganglion cells, inner plexiform layer, and photoreceptor–RPE zone.⁶⁹ Ultrastructural analysis revealed storage material in the ganglion, bipolar, and photoreceptor cells of 12- and 18-month-old mutant mice,⁶⁹ who showed loss of retinal ganglion cell axons, axonal hypertrophy, and reduced myelination.^{61,70} Further phenotypic analyses of these mice demonstrated decreased optic nerve conduction, reduced neuron numbers in the LGNd, and defective amino acid transport from the retina to the LGNd.⁷¹ Evaluation of global gene expression in the whole eyes, but not in the cerebellum, of these mice prior to the appearance of lysosomal deposits showed significant downregulation of genes associated with energy production in the mitochondria, including cytochrome *b*, cytochrome oxidase, and mitochondrial ATP synthase F₀ complex subunit B.⁶⁸ This finding is consistent with accumulation of mitochondrial ATPase F₀ complex subunit *c* in the storage material and reduced mitochondrial ATP hydrolysis in JNCL skin fibroblasts.^{30–32} Most recently, RPE of these mutant mice have been reported for the first time to also contain mitochondrial ATPase F₀ complex subunit *c*-positive storage material and to have defective autolysosomal degradation and photoreceptor phagosome processing.⁷² In addition, toluidine blue-staining of optic nerves showed mast cell infiltration in the *Cln3*-deficient mice in comparison to wild-type mice, suggesting inflammation and a defective BBB.⁶¹ Furthermore, at 5 months of age, these mice showed low levels of glial cell activation (without evidence of complete activation of microglia and astrocytes) in the brain, including in the visual cortex, where low glial cell activation preceded the neuronal damage by many months.⁷³ However, inflammation or gliosis has not been specifically examined in the retina. Although this mouse model generally recapitulates the human pathologies of JNCL quite well, the extent of retinal degeneration and functional visual impairment by fundus examination and ERG at 11 months of age is not as extensive as in JNCL patients.⁶⁹

In the second mouse model (*Cln3^{ex7/8}* knock-out; generated in 129X1/SvJ RW4 mouse ES cells and backcrossed to C57BL/6J mice), most of exon 7 and all of exon 8 were deleted;⁷⁴ these mice had a significantly shortened lifespan in comparison with wild-type littermates (by 19% of mean lifespan and 30% of maximum lifespan).⁷⁵ Autofluorescent storage bodies were abundant in the cerebral cortex and liver by 15 weeks of age.⁷⁴ The amount of autofluorescent storage material was substantially greater in the brain, neural retina, and RPE at the ages of 12 months of age or older. Neurological signs, such as defects in associative learning, started as early as 14 weeks of age, while no significant alterations in the ERG responses (e.g., scotopic a- and b-wave amplitudes) were observed in the mutant mice at this age.⁷⁶ At either 12- or 24-months of age, scotopic b-wave amplitudes of the mutant mice were significantly reduced as compared to those of wild-type mice, while a-wave amplitudes did not differ significantly between the mutant and wild-type mice. These results suggest that the functional deficits are more restricted to the inner nuclear layer of retina than to photoreceptors.⁷⁵ Consistently, at both 12 and 24 months of age, substantial loss of nucleated cells in the inner nuclear layer (but not in the photoreceptor cell layer) and

ganglion cells (assessed by optic nerve axon numbers and cross-sectional area) were noted.⁷⁵ However, photopic b-wave amplitudes recorded under rod-suppressing conditions were significantly reduced in the mutant mice compared to their wild-type littermates at both 12 and 24 months of age,⁷⁵ suggesting significant cone dysfunction.

The third JNCL mouse model (*Cln3*^{ex7/8} knock-in; generated in 129X1 × 129S1 progeny R1 ES cells) mimics the most common *Cln3* mutation (i.e., 1 kb deletion in exons 7 and 8) in patients with JNCL.⁷⁷ On an outbred 129Sv/Ev/CD1 background, this mouse model had reduced *Cln3* mRNA levels as well as several alternatively spliced mRNAs, which is consistent with the human disease. Mortality starts at 7 months of age, with the survival rate reaching 80% by 10–12 months.⁷⁷ Deposition of the mitochondrial ATPase F₀ complex subunit *c*-immunoreactive autofluorescent storage material was widespread—most prominently in the liver and selective regions of the nervous system, including the retinal ganglion cell layer, inner nuclear layer, and to a lesser degree, the outer nuclear layer.^{77, 78} As shown by electron microscopy, *Cln3*^{ex7/8} mice showed abundant perinuclear inclusions with the classic fingerprint profiles in the cytoplasm of retinal ganglion cells (Fig. 3C).⁷⁷ Interestingly, liver function and neural development were normal, despite development of extensive mitochondrial ATPase subunit *c*-reactive deposits in the liver, cerebellar Purkinje cells, dentate gyrus, and subventricular zone at E19.5 (disappeared by P8 in the latter two regions). At P1.5, these mutant mice developed small deposits in the neuroblastic layer (NBL) of the retina, which became evident by P8 when the NBL matured into the inner and outer nuclear layers. By 10 months of age, there was significant retinal hypopigmentation and associated reduction in cone cell density in *Cln3*^{ex7/8} mice.⁷⁷ *Cln3*^{ex7/8} mice also showed striking reactive gliosis in the cerebral cortex and white matter by as early as 3 months old.^{77, 78} On both C57BL/6N⁷⁹ and C57BL/6⁸⁰ background, there was a small but significant reduction in photopic ERG amplitudes by the age of 5–6 months, suggesting early loss of cone function.^{79, 80} By the age of 9 months, a small but significant and selective loss of b-wave amplitudes in the scotopic ERG occurred without any change in a-wave amplitudes, suggesting decreased functions of postsynaptic retinal neurons in the inner retina.^{79, 80} On a C57BL/6N background, the central nervous system behavioral defects appeared to precede ocular visual system behavioral defects: an approximately 3-day delay of negative geotaxis and the grasping reflex was observed during preweaning neurodevelopment, and at 8 weeks old, exploratory behaviors (as monitored by the open-field test) were reduced, motor deficits were apparent (as assessed by rotarod and gait analyses) without anxiety- or depression-like behaviors (as assessed by elevated plus maze and forced swimming test, respectively), or marked visual impairment (as assessed by Morris water maze with visual clues) in *Cln3*^{ex7/8} mice.⁸¹

In vitro, conditionally immortalized neurons from the *Cln3*^{ex7/8} knock-in mouse model have been used as a cerebellar neuronal precursor cell model.⁸² These mutant cells expressed low levels of mutant Cln3 protein and accumulated the mitochondrial ATPase F₀ complex subunit *c*. These cells demonstrated endosomal/lysosomal trafficking defects, structural and functional abnormalities in mitochondria, and decreased cell survival in response to oxidative stress.⁸² These trafficking defects and mitochondrial dysfunctions preceded subunit *c* deposition.

Macroautophagy (referred to here as autophagy) is an essential lysosomal degradation pathway that involves *de novo* biogenesis of autophagosomes for packaging and trafficking of luminal cargos, including mitochondria to lysosomes for degradation. The CLN3 protein was reported to interact with the core autophagy protein Atg7 in 293T cells,⁸³ and mouse Cln3 protein was highly enriched in the subcellular fractions containing autophagic vacuoles,⁷⁷ suggesting that Cln3 may function in the autophagy pathway. Further studies using the *Cln3*^{ex7/8} knock-in mouse model and the derived cerebellar neuronal precursor cell model showed upregulation of the autophagosome marker LC3-II (by immunohistochemistry in the brain sections corresponding to the regions known for mitochondrial ATPase F₀ complex subunit *c* accumulation and by Western blotting of whole-brain extracts) and autophagy-inducing, down-regulation of mammalian target of rapamycin (mTOR) complex 1 activity.⁸⁴ Ultrastructural analysis of purified autophagic vacuoles from homozygous *Cln3*^{ex7/8} knock-in mutants and their wild-type littermates also pointed to likely defects in autophagic vacuolar maturation and in trafficking between endosomal and lysosomal compartments.⁸⁴ Therefore, data collected from the *Cln3*^{ex7/8} knock-in mouse model suggest that defects in endosomal/lysosomal trafficking, including the autophagy pathway, likely contribute to JNCL pathogenesis.

Non-murine models of JNCL

Yeast,^{85–91} *Caenorhabditis elegans*,⁹² *Drosophila*,⁹³ and *Dictyostelium discoideum*⁹⁴ models of JNCL generated by manipulation of *CLN3* orthologs are currently available. These non-mammalian models may provide important clues to CLN3 function. A promising attempt in the generation of a porcine model of JNCL specifically targeting the *Cln3* gene is ongoing.⁹⁵ Once available, this porcine model will be especially useful for evaluating early-stage ocular phenotypes to overcome the difficulties in recapitulating human JNCL pathological features in mice.

Ocular pathologies in other lysosomal storage disorders

Ocular pathologies are common in all childhood forms of NCLs, with retina atrophy more pronounced in INCL and JNCL than in LINCL and its variants.^{96, 97} Importantly, retinal degeneration in these NCLs starts at the photoreceptor outer segments and proceeds inward during the disease progression.^{96, 97} Ocular manifestations including corneal and/or vitreous opacities, as well as retinal pigmentary changes, have also been reported in non-NCL lysosomal storage disorders.⁹⁸ Specifically, retinal phenotypes are prominent in Gaucher disease (retinal vascular tortuosity),⁹⁹ Niemann–Pick disease (macular halos and cherry-red spots in the macula),¹⁰⁰ Fabry's disease (tortuous and aneurysmal dilatations of retinal vessels),¹⁰¹ Tay–Sachs disease and Sandhoff disease (both with cherry-red spots in the macula and optic atrophy),¹⁰² Krabbe disease (pale optic discs),¹⁰³ metachromatic leukodystrophy (foveal atrophy with chorio-retinal atrophy and progressive retinal pigment degeneration),¹⁰⁴ mucopolysaccharidosis (RPE atrophy and optic disc pallor with ERG changes),¹⁰⁵ and mucopolisaccharidosis and sialidosis (both with cherry-red spots in the macula).^{106, 107} In addition, the widely used antimalarial and anti-inflammatory drugs chloroquine (CQ) and hydroxychloroquine (HCQ), which block lysosomal acidification and

degradation, have side effects including retinopathy (bull's eye maculopathy) and vision loss.^{108, 109}

Discussion and future directions

As the earliest symptom of JNCL that often brings patients into the clinic, vision impairment presents an invaluable opportunity for intervention before the development of irreversible retinal degeneration and neurodegeneration. Moreover, an understanding of the pathophysiology of vision loss in JNCL may shed light on the systemic manifestations of the disease. In addition, using next-generation sequencing, *CLN3* was recently identified as a novel non-syndromic retinal disease gene, with all patients who carry these mutations showing retinal degeneration phenotypes without additional signs of JNCL.¹¹⁰ This suggests that there likely are factors independent of neurodegeneration contributing to JNCL vision loss. However, despite the importance of understanding early vision failure in JNCL, the mechanisms underlying vision loss in JNCL remain poorly understood.

We have yet to identify the primary cells in which the ocular pathologies are initiated in JNCL and the sequence of events during the progression of vision impairment. The retinal phenotypes in mouse models appear to be mostly limited to the inner retina and optic nerve, even though there is deposition of lipopigments in other cells such as RPE. However, JNCL patients clearly show prominent RPE atrophy of macula and have significant loss of RPE cells, suggesting that JNCL mutations of *CLN3* may result in tissue- and cell-specific disease manifestations, possibly associated with tissue- and cell-specific patterns of *CLN3/Cln3* expression, as shown in the *Cln3^{LacZ/LacZ}* mouse model.^{63, 64} It is also plausible that damage to the inner retinal cells may be secondary to retrograde damage from functional impairment in the outer retinal cells, including rods, cones, and RPE. We are currently investigating the effects of *CLN3/Cln3* deficiency in RPE, photoreceptors, and inner retinal neurons, both *in vitro* and *in vivo*. In addition, the normal functions of *CLN3* and the importance of lipopigment accumulation resulting from JNCL mutations are unclear at this time. These questions call for the production of critical reagents (e.g., high-affinity and high-specificity antibodies that can recognize endogenous *CLN3/Cln3* proteins), identification of the molecular compositions of the deposit, determination of retina cell type-specific functions of wild-type *CLN3/Cln3* protein for normal vision, and thorough characterization of ocular pathologies of JNCL mutations in human patients and other species.

Another major hurdle in understanding JNCL disease etiology and design therapeutics is the discrepancy in ocular phenotypes between human patients and mouse models: unlike what is seen in available mouse models, JNCL patients develop vision loss as one of the earliest clinical symptoms. These patients have severe ERG abnormalities and retinal degeneration early in the disease process. In contrast, the mouse ocular pathologies occur relatively late and photoreceptors in these models appear to be relatively well preserved. The underlying reasons for this difference in the staging and severity of disease features are not known, but several possibilities exist. First, intrinsic short life span of mice is possibly the main deterrent for the development of well-evolved retinal degeneration. Second, the human and mouse retina has distinct anatomy: cones are responsible for clear vision during the day, while rods are responsible for vision in low light and for peripheral vision. Unlike humans,

mice are nocturnal, with rods functioning as the dominant photoreceptor (> 95%) and with much fewer cones in the retina.^{111, 112} Moreover, mice do not have a central macula or fovea, where many initial anatomical findings associated with JNCL (e.g., the bull's eye maculopathy) are located. Third, mice may have compensatory mechanisms that ameliorate JNCL and may provide hints to potential therapeutics. Finally, there may be an environmental component that is different in humans versus mice and that interacts with the *CLN3/Cln3* gene to affect disease onset and progression.

With regard to the current mouse models, there are several confounding issues that require continued investigation. The CD1 background mice are susceptible to native retinal degeneration genetic loci that are independent of the *Cln3* locus, leaving the interpretation of the original characterization of retinal degeneration in the *Cln3^{ex7/8}* knock-in mouse model in question.⁷⁹ Genetic background, gender, and age have been shown recently in a systematic study to affect exploratory activity, motor function, and depressive-like behaviors in *Cln^{-/-}* and *Cln3^{ex7/8}* knock-in mouse models of JNCL.¹¹³ Similar systematic comparisons are needed in order to characterize the ocular pathologies in JNCL mouse models.

Given the complexities encountered in the development of a reliable animal model, alternative approaches should be considered to study this disease. For instance, a recent study using the induced pluripotent stem cell (iPSC) model from JNCL patients revealed impairment in autophagic clearance and ultrastructural defects in late endosomal–lysosomal compartments, multivesicular bodies, mitochondria, Golgi, and endoplasmic reticulum in neurons derived from these iPSC clones.¹¹⁴ Development of such models (e.g., retina cell-specific iPSC clones) will help advance our current knowledge on the etiology of JNCL vision loss and facilitate future drug screening.

Research on the genetic basis of JNCL needs to be translated into therapies aimed at preventing and improving ocular and neuronal defects in JNCL patients. For prevention, though attempts to develop antenatal screening tests using next-generation sequencing are promising, no commercial products are currently available.¹¹⁵ For treatment, gene therapy using adeno-associated virus (AAV)–mediated *CLN3* delivery has shown to partially reverse biochemical and pathological defects in a murine model of JNCL.¹¹⁶ Intracranial delivery of AAV is a common method used for treating neurological disorders, including Parkinson's, Canavan's, and Alzheimer's diseases. In fact, a phase I study is ongoing for gene transfer–based therapy for treating LINCL (CLN2 disease).¹¹⁷ Given the promising results of AAV-mediated *CLN3* delivery in a JNCL mouse model¹¹⁶ and the ongoing gene therapy trial for treating CLN2 disease, a gene therapy trial for treating CLN3 disease is likely to be on the horizon. In other avenues of treatment, there are ongoing phase II/III trials to assess the utility of anti-inflammatory agents¹¹⁸ and stem cell transplant.¹¹⁹ The former is based on earlier studies where (1) autoantibodies to different neuronal components, including glutamic acid decarboxylase, have been identified in both JNCL patients^{40–43} and *Cln3^{-/-}* mice,^{40, 43} and (2) either genetic (μ MT mice with B cell deficiency) or pharmacological (using the immunosuppressant mycophenolate mofetil) intervention reduced neuroinflammatory responses, and importantly, improved motor performance.¹²⁰ Further studies aimed at elucidating molecular mechanisms underlying the functions of

CLN3 will promote the identification of novel therapeutics for ultimately improving the quality of life of JNCL patients and curing this devastating disease.

Acknowledgments

This work was supported by the Ellison Medical Foundation and startup funds from the University of Kentucky (to Q.J.W.). Other support includes NIH Grant K08EY021757, a Foundation Fighting Blindness Career Development Award, and a Research to Prevent Blindness Career Development Award (all to M.E.K.). The authors thank Dr. Dean Hainsworth for providing the high-quality image from his original publication. We apologize to those authors whose work could not be cited because of space limitations.

References

1. Pérez-Poyato MS, et al. Juvenile neuronal ceroid lipofuscinosis: clinical course and genetic studies in Spanish patients. *J Inherit Metab Dis*. 2011; 34:1083–1093. [PubMed: 21499717]
2. Cialone J, et al. Females experience a more severe disease course in Batten disease. *Journal of inherited metabolic disease*. 2012; 35:549–555. [PubMed: 22167274]
3. Nielsen AK, Ostergaard JR. Do females with juvenile ceroid lipofuscinosis (Batten disease) have a more severe disease course? The Danish experience. *Eur J Paediatr Neurol*. 2013; 17:265–268. [PubMed: 23177590]
4. Batten FE. Cerebral degeneration with symmetrical changes in the maculae in two members of a family. *Trans Ophthalmol Soc UK*. 1903; 23:386–390.
5. Williams RE, Mole SE. New nomenclature and classification scheme for the neuronal ceroid lipofuscinoses. *Neurology*. 2012; 79:183–191. [PubMed: 22778232]
6. Mink JW, et al. Classification and natural history of the neuronal ceroid lipofuscinoses. *J Child Neurol*. 2013; 28:1101–1105. [PubMed: 23838030]
7. The-International-Batten-Disease-Consortium. Isolation of a novel gene underlying Batten disease, CLN3. *Cell*. 1995; 82:949–957. [PubMed: 7553855]
8. Uvebrant P, Hagberg B. Neuronal ceroid lipofuscinoses in Scandinavia. *Epidemiology and clinical pictures. Neuropediatrics*. 1997; 28:6–8. [PubMed: 9151309]
9. Cotman SL, et al. Neuronal ceroid lipofuscinosis: impact of recent genetic advances and expansion of the clinicopathologic spectrum. *Curr Neurol Neurosci Rep*. 2013; 13:366. [PubMed: 23775425]
10. Pearce DA. Localization and processing of CLN3, the protein associated to Batten disease: where is it and what does it do? *J Neurosci Res*. 2000; 59:19–23. [PubMed: 10658181]
11. Phillips SN, et al. CLN3, the protein associated with batten disease: structure, function and localization. *J Neurosci Res*. 2005; 79:573–583. [PubMed: 15657902]
12. Kyttälä A, et al. Functional biology of the neuronal ceroid lipofuscinoses (NCL) proteins. *Biochim Biophys Acta*. 2006; 1762:920–933. [PubMed: 16839750]
13. Järvelä I, et al. Defective intracellular transport of CLN3 is the molecular basis of Batten disease (JNCL). *Hum Mol Genet*. 1999; 8:1091–1098. [PubMed: 10332042]
14. Kida E, et al. Analysis of intracellular distribution and trafficking of the CLN3 protein in fusion with the green fluorescent protein in vitro. *Mol Genet Metab*. 1999; 66:265–271. [PubMed: 10191113]
15. Golabek AA, et al. Expression studies of CLN3 protein (battenin) in fusion with the green fluorescent protein in mammalian cells in vitro. *Mol Genet Metab*. 1999; 66:277–282. [PubMed: 10191115]
16. Ezaki J, et al. Characterization of Cln3p, the gene product responsible for juvenile neuronal ceroid lipofuscinosis, as a lysosomal integral membrane glycoprotein. *J Neurochem*. 2003; 87:1296–1308. [PubMed: 14622109]
17. Kyttälä A, et al. Two motifs target Batten disease protein CLN3 to lysosomes in transfected nonneuronal and neuronal cells. *Mol Biol Cell*. 2004; 15:1313–1323. [PubMed: 14699076]
18. Järvelä I, et al. Biosynthesis and intracellular targeting of the CLN3 protein defective in Batten disease. *Hum Mol Genet*. 1998; 7:85–90. [PubMed: 9384607]

19. Luiro K, et al. Interconnections of CLN3, Hook1 and Rab proteins link Batten disease to defects in the endocytic pathway. *Hum Mol Genet.* 2004; 13:3017–3027. [PubMed: 15471887]
20. Haskell RE, et al. Batten disease: evaluation of CLN3 mutations on protein localization and function. *Hum Mol Genet.* 2000; 9:735–744. [PubMed: 10749980]
21. Munroe PB, et al. Spectrum of mutations in the Batten disease gene, CLN3. *Am J Hum Genet.* 1997; 61:310–316. [PubMed: 9311735]
22. Kitzmuller C, et al. A function retained by the common mutant CLN3 protein is responsible for the late onset of juvenile neuronal ceroid lipofuscinosis. *Hum Mol Genet.* 2008; 17:303–312. [PubMed: 17947292]
23. Rakheja D, Narayan SB, Bennett MJ. Juvenile neuronal ceroid-lipofuscinosis (Batten disease): a brief review and update. *Curr Mol Med.* 2007; 7:603–608. [PubMed: 17896996]
24. Autti T, et al. Thalami and corona radiata in juvenile NCL (CLN3): a voxel-based morphometric study. *Eur J Neurol.* 2007; 14:447–450. [PubMed: 17388996]
25. Autti TH, et al. JNCL patients show marked brain volume alterations on longitudinal MRI in adolescence. *J Neurol.* 2008; 255:1226–1230. [PubMed: 18677643]
26. Tokola AM, et al. Hippocampal volumes in juvenile neuronal ceroid lipofuscinosis: a longitudinal magnetic resonance imaging study. *Pediatr Neurol.* 2014; 50:158–163. [PubMed: 24411222]
27. Dyken PR. Reconsideration of the classification of the neuronal ceroid-lipofuscinoses. *Am J Med Genet Suppl.* 1988; 5:69–84. [PubMed: 3146331]
28. Wisniewski KE, Rapin I, Heaney-Kieras J. Clinico-pathological variability in the childhood neuronal ceroid-lipofuscinoses and new observations on glycoprotein abnormalities. *Am J Med Genet Suppl.* 1988; 5:27–46. [PubMed: 3146325]
29. Henry JG, Stevens SM. Neuronal ceroid lipofuscinosis in the amaurotic retardate: electron microscopic confirmation. *Aust J Ophthalmol.* 1982; 10:161–166. [PubMed: 7181756]
30. Hall NA, et al. Lysosomal storage of subunit c of mitochondrial ATP synthase in Batten's disease (ceroid-lipofuscinosis). *Biochem J.* 1991; 275(Pt 1):269–272. [PubMed: 1826833]
31. Palmer DN, et al. Mitochondrial ATP synthase subunit c storage in the ceroid-lipofuscinoses (Batten disease). *Am J Med Genet.* 1992; 42:561–567. [PubMed: 1535179]
32. Das AM, Kohlschutter A. Decreased activity of the mitochondrial ATP-synthase in fibroblasts from children with late-infantile and juvenile neuronal ceroid lipofuscinosis. *J Inherit Metab Dis.* 1996; 19:130–132. [PubMed: 8739947]
33. Bozorg S, et al. Juvenile neuronal ceroid lipofuscinosis (JNCL) and the eye. *Surv Ophthalmol.* 2009; 54:463–471. [PubMed: 19539834]
34. Ostergaard JR, Rasmussen TB, Mølgaard H. Cardiac involvement in juvenile neuronal ceroid lipofuscinosis (Batten disease). *Neurology.* 2011; 76:1245–1251. [PubMed: 21464428]
35. Murata S, et al. Juvenile neuronal ceroid-lipofuscinosis with hypertrophic cardiomyopathy and left ventricular noncompaction: a case report. *Rinsho shinkeigaku = Clinical neurology.* 2014; 54:38–45. [PubMed: 24429647]
36. Fukumura S, et al. Progressive conduction defects and cardiac death in late infantile neuronal ceroid lipofuscinosis. *Dev Med Child Neurol.* 2012; 54:663–666. [PubMed: 22221116]
37. Hofman IL, et al. Cardiac pathology in neuronal ceroid lipofuscinoses--a clinicopathologic correlation in three patients. *Eur J Paediatr Neurol.* 2001; 5(Suppl A):213–217. [PubMed: 11589001]
38. Lebrun AH, et al. Analysis of potential biomarkers and modifier genes affecting the clinical course of CLN3 disease. *Mol Med.* 2011; 17:1253–1261. [PubMed: 21863212]
39. Carlen B, Englund E. Diagnostic value of electron microscopy in a case of juvenile neuronal ceroid lipofuscinosis. *Ultrastruct Pathol.* 2001; 25:285–288. [PubMed: 11577772]
40. Chattopadhyay S, et al. An autoantibody inhibitory to glutamic acid decarboxylase in the neurodegenerative disorder Batten disease. *Hum Mol Genet.* 2002; 11:1421–1431. [PubMed: 12023984]
41. Chattopadhyay S, et al. An autoantibody to GAD65 in sera of patients with juvenile neuronal ceroid lipofuscinoses. *Neurology.* 2002; 59:1816–1817. [PubMed: 12473787]

42. Lim MJ, et al. Distinct patterns of serum immunoreactivity as evidence for multiple brain-directed autoantibodies in juvenile neuronal ceroid lipofuscinosis. *Neuropathol Appl Neurobiol.* 2006; 32:469–482. [PubMed: 16972881]
43. Lim MJ, et al. IgG entry and deposition are components of the neuroimmune response in Batten disease. *Neurobiol Dis.* 2007; 25:239–251. [PubMed: 17070688]
44. Conradi NG, et al. First-trimester diagnosis of juvenile neuronal ceroid lipofuscinosis by demonstration of fingerprint inclusions in chorionic villi. *Prenat Diagn.* 1989; 9:283–287. [PubMed: 2541423]
45. Spalton DJ, Taylor DS, Sanders MD. Juvenile Batten's disease: an ophthalmological assessment of 26 patients. *Br J Ophthalmol.* 1980; 64:726–732. [PubMed: 7426545]
46. Collins J, et al. Batten disease: features to facilitate early diagnosis. *Br J Ophthalmol.* 2006; 90:1119–1124. [PubMed: 16754648]
47. Hainsworth DP, et al. Funduscopy and angiographic appearance in the neuronal ceroid lipofuscinoses. *Retina.* 2009; 29:657–668. [PubMed: 19289983]
48. Goebel HH, Fix JD, Zeman W. The fine structure of the retina in neuronal ceroid-lipofuscinosis. *Am J Ophthalmol.* 1974; 77:25–39. [PubMed: 4824171]
49. Seeliger M, et al. Juvenile neuronal ceroid lipofuscinosis (Batten-Mayou) disease. Ophthalmologic diagnosis and findings. *Ophthalmologie.* 1997; 94:557–562. [PubMed: 9376693]
50. Weleber RG. The dystrophic retina in multisystem disorders: the electroretinogram in neuronal ceroid lipofuscinoses. *Eye (Lond).* 1998; 12(Pt 3b):580–590. [PubMed: 9775220]
51. Eksandh LB, et al. Full-field ERG in patients with Batten/Spielmeier-Vogt disease caused by mutations in the CLN3 gene. *Ophthalmic Genet.* 2000; 21:69–77. [PubMed: 10916181]
52. Krohne TU, et al. Juvenile neuronal ceroid lipofuscinosis. Ophthalmologic findings and differential diagnosis. *Ophthalmologie.* 2010; 107:606–611. [PubMed: 20454901]
53. Nielsen AK, Drack AV, Ostergaard JR. Cataract and glaucoma development in juvenile neuronal ceroid lipofuscinosis (batten disease). *Ophthalmic Genet.* 2015; 36:39–42. [PubMed: 25365415]
54. Bensaoula T, et al. Histopathologic and immunocytochemical analysis of the retina and ocular tissues in Batten disease. *Ophthalmology.* 2000; 107:1746–1753. [PubMed: 10964839]
55. Katz ML, Rodrigues M. Juvenile ceroid lipofuscinosis. Evidence for methylated lysine in neural storage body protein. *Am J Pathol.* 1991; 138:323–332. [PubMed: 1899540]
56. Drack AV, et al. Immunosuppressive treatment for retinal degeneration in juvenile neuronal ceroid lipofuscinosis (juvenile Batten disease). *Ophthalmic Genet.* 2014:1–6. Online.
57. Birch DG. Retinal degeneration in retinitis pigmentosa and neuronal ceroid lipofuscinosis: An overview. *Mol Genet Metab.* 1999; 66:356–366. [PubMed: 10191129]
58. Hansen MS, et al. Optical Coherence Tomography in Juvenile Neuronal Ceroid Lipofuscinosis. *Retin Cases Brief Rep.* 2015
59. Dulz S, et al. Novel morphological macular findings in juvenile CLN3 disease. *Br J Ophthalmol.* 2015:1–5. Online. [PubMed: 24879806]
60. Katz ML, et al. Immunochemical localization of the Batten disease (CLN3) protein in retina. *Invest Ophthalmol Vis Sci.* 1997; 38:2375–2386. [PubMed: 9344361]
61. Sappington RM, Pearce DA, Calkins DJ. Optic nerve degeneration in a murine model of juvenile ceroid lipofuscinosis. *Invest Ophthalmol Vis Sci.* 2003; 44:3725–3731. [PubMed: 12939285]
62. Getty AL, Pearce DA. Interactions of the proteins of neuronal ceroid lipofuscinosis: clues to function. *Cell Mol Life Sci.* 2011; 68:453–474. [PubMed: 20680390]
63. Eliason SL, et al. A knock-in reporter model of Batten disease. *J Neurosci.* 2007; 27:9826–9834. [PubMed: 17855597]
64. Ding SL, et al. A knock-in reporter mouse model for Batten disease reveals predominant expression of Cln3 in visual, limbic and subcortical motor structures. *Neurobiology of disease.* 2011; 41:237–248. [PubMed: 20875858]
65. Tecedor L, et al. CLN3 loss disturbs membrane microdomain properties and protein transport in brain endothelial cells. *J Neurosci.* 2013; 33:18065–18079. [PubMed: 24227717]
66. Greene ND, et al. A murine model for juvenile NCL: gene targeting of mouse Cln3. *Mol Genet Metab.* 1999; 66:309–313. [PubMed: 10191119]

67. Mitchison HM, et al. Targeted disruption of the *Cln3* gene provides a mouse model for Batten disease. The Batten Mouse Model Consortium [corrected]. *Neurobiol Dis.* 1999; 6:321–334. [PubMed: 10527801]
68. Chattopadhyay S, et al. Altered gene expression in the eye of a mouse model for batten disease. *Invest Ophthalmol Vis Sci.* 2004; 45:2893–2905. [PubMed: 15326100]
69. Seigel GM, et al. Retinal pathology and function in a *Cln3* knockout mouse model of juvenile Neuronal Ceroid Lipofuscinosis (batten disease). *Mol Cell Neurosci.* 2002; 19:515–527. [PubMed: 11988019]
70. Mitchison HM, Lim MJ, Cooper JD. Selectivity and types of cell death in the neuronal ceroid lipofuscinoses. *Brain Pathol.* 2004; 14:86–96. [PubMed: 14997941]
71. Weimer JM, et al. Visual deficits in a mouse model of Batten disease are the result of optic nerve degeneration and loss of dorsal lateral geniculate thalamic neurons. *Neurobiol Dis.* 2006; 22:284–293. [PubMed: 16412658]
72. Wavre-Shapton ST, et al. Photoreceptor phagosome processing defects and disturbed autophagy in retinal pigment epithelium of *Cln3Deltaex1-6* mice modelling juvenile neuronal ceroid lipofuscinosis (Batten disease). *Hum Mol Genet.* 2015:1–15. Online.
73. Pontikis CC, et al. Late onset neurodegeneration in the *Cln3*–/– mouse model of juvenile neuronal ceroid lipofuscinosis is preceded by low level glial activation. *Brain Res.* 2004; 1023:231–242. [PubMed: 15374749]
74. Katz ML, et al. A mouse gene knockout model for juvenile ceroid-lipofuscinosis (Batten disease). *J Neurosci Res.* 1999; 57:551–556. [PubMed: 10440905]
75. Katz ML, et al. Phenotypic characterization of a mouse model of juvenile neuronal ceroid lipofuscinosis. *Neurobiol Dis.* 2008; 29:242–253. [PubMed: 17962032]
76. Wendt KD, et al. Behavioral assessment in mouse models of neuronal ceroid lipofuscinosis using a light-cued T-maze. *Behav Brain Res.* 2005; 161:175–182. [PubMed: 15885820]
77. Cotman SL, et al. *Cln3(Deltaex7/8)* knock-in mice with the common JNCL mutation exhibit progressive neurologic disease that begins before birth. *Hum Mol Genet.* 2002; 11:2709–2721. [PubMed: 12374761]
78. Herrmann P, et al. Developmental impairments of select neurotransmitter systems in brains of *Cln3(Deltaex7/8)* knock-in mice, an animal model of juvenile neuronal ceroid lipofuscinosis. *J Neurosci Res.* 2008; 86:1857–1870. [PubMed: 18265413]
79. Staropoli JF, et al. Large-scale phenotyping of an accurate genetic mouse model of JNCL identifies novel early pathology outside the central nervous system. *PLoS One.* 2012; 7:e38310. [PubMed: 22701626]
80. Volz C, et al. Retinal function in aging homozygous *Cln3 (Deltaex7/8)* knock-in mice. *Adv Exp Med Biol.* 2014; 801:495–501. [PubMed: 24664736]
81. Osório NS, et al. Neurodevelopmental delay in the *Cln3Deltaex7/8* mouse model for Batten disease. *Genes Brain Behav.* 2009; 8:337–345. [PubMed: 19243453]
82. Fossale E, et al. Membrane trafficking and mitochondrial abnormalities precede subunit c deposition in a cerebellar cell model of juvenile neuronal ceroid lipofuscinosis. *BMC Neurosci.* 2004; 5:57. [PubMed: 15588329]
83. Behrends C, et al. Network organization of the human autophagy system. *Nature.* 2010; 466:68–76. [PubMed: 20562859]
84. Cao Y, et al. Autophagy is disrupted in a knock-in mouse model of juvenile neuronal ceroid lipofuscinosis. *J Biol Chem.* 2006; 281:20483–20493. [PubMed: 16714284]
85. Pearce DA, et al. Action of *BTN1*, the yeast orthologue of the gene mutated in Batten disease. *Nat Genet.* 1999; 22:55–58. [PubMed: 10319861]
86. Pearce DA, et al. Phenotypic reversal of the *btn1* defects in yeast by chloroquine: a yeast model for Batten disease. *Proc Natl Acad Sci U S A.* 1999; 96:11341–11345. [PubMed: 10500178]
87. Kim Y, Ramirez-Montealegre D, Pearce DA. A role in vacuolar arginine transport for yeast *Btn1p* and for human *CLN3*, the protein defective in Batten disease. *Proc Natl Acad Sci U S A.* 2003; 100:15458–15462. [PubMed: 14660799]

88. Codlin S, et al. Btn1 affects cytokinesis and cell-wall deposition by independent mechanisms, one of which is linked to dysregulation of vacuole pH. *J Cell Sci.* 2008; 121:2860–2870. [PubMed: 18697832]
89. Codlin S, Mole SE. S. pombe btn1, the orthologue of the Batten disease gene CLN3, is required for vacuole protein sorting of Cpy1p and Golgi exit of Vps10p. *J Cell Sci.* 2009; 122:1163–1173. [PubMed: 19299465]
90. Kama R, et al. The yeast Batten disease orthologue Btn1 controls endosome-Golgi retrograde transport via SNARE assembly. *J Cell Biol.* 2011; 195:203–215. [PubMed: 21987636]
91. Chattopadhyay S, Roberts PM, Pearce DA. The yeast model for Batten disease: a role for Btn2p in the trafficking of the Golgi-associated vesicular targeting protein, Yif1p. *Biochem Biophys Res Commun.* 2003; 302:534–538. [PubMed: 12615067]
92. de Voer G, et al. Deletion of the *Caenorhabditis elegans* homologues of the CLN3 gene, involved in human juvenile neuronal ceroid lipofuscinosis, causes a mild progeric phenotype. *J Inherit Metab Dis.* 2005; 28:1065–1080. [PubMed: 16435200]
93. Tuxworth RI, et al. The Batten disease gene CLN3 is required for the response to oxidative stress. *Hum Mol Genet.* 2011; 20:2037–2047. [PubMed: 21372148]
94. Huber RJ, Myre MA, Cotman SL. Loss of Cln3 function in the social amoeba *Dictyostelium discoideum* causes pleiotropic effects that are rescued by human CLN3. *PLoS One.* 2014; 9:e110544. [PubMed: 25330233]
95. Rogers C. Development of a porcine model of juvenile neuronal ceroid. 2013
96. Anderson GW, Goebel HH, Simonati A. Human pathology in NCL. *Biochim Biophys Acta.* 2013; 1832:1807–1826. [PubMed: 23200925]
97. Radke J, Stenzel W, Goebel HH. Human NCL Neuropathology. *Biochim Biophys Acta.* 2015
98. Biswas J, et al. Ocular manifestation of storage diseases. *Current opinion in ophthalmology.* 2008; 19:507–511. [PubMed: 18854696]
99. Shrier EM, Barr CC, Grabowski GA. Vitreous opacities and retinal vascular abnormalities in Gaucher disease. *Arch Ophthalmol.* 2004; 122:1395–1398. [PubMed: 15364726]
100. McGovern MM, et al. Ocular manifestations of Niemann-Pick disease type B. *Ophthalmology.* 2004; 111:1424–1427. [PubMed: 15234149]
101. Sodi A, et al. Ocular manifestations of Fabry's disease: data from the Fabry Outcome Survey. *Br J Ophthalmol.* 2007; 91:210–214. [PubMed: 16973664]
102. Brady RO. Ophthalmologic aspects of lipid storage diseases. *Ophthalmology.* 1978; 85:1007–1013. [PubMed: 105334]
103. Harcourt B, Ashton N. Ultrastructure of the optic nerve in Krabbe's leucodystrophy. *Br J Ophthalmol.* 1973; 57:885–891. [PubMed: 4788949]
104. Weiter JJ, et al. Retinal pigment epithelial degeneration associated with leukocytic arylsulfatase A deficiency. *American journal of ophthalmology.* 1980; 90:768–772. [PubMed: 6108718]
105. Ashworth JL, et al. The ocular features of the mucopolysaccharidoses. *Eye (Lond).* 2006; 20:553–563. [PubMed: 15905869]
106. Riedel KG, et al. Ocular abnormalities in mucopolidosis IV. *American journal of ophthalmology.* 1985; 99:125–136. [PubMed: 3918453]
107. Kirkham TH, Coupland SG, Guitton D. Sialidosis: the cherry-red spot--myoclonus syndrome. *Can J Ophthalmol.* 1980; 15:35–39. [PubMed: 7378886]
108. Korthagen NM, et al. Chloroquine and Hydroxychloroquine Increase Retinal Pigment Epithelial Layer Permeability. *J Biochem Mol Toxicol.* 2015; 29:299–304. [PubMed: 25752684]
109. Tzekov R. Ocular toxicity due to chloroquine and hydroxychloroquine: electrophysiological and visual function correlates. *Doc Ophthalmol.* 2005; 110:111–120. [PubMed: 16249962]
110. Wang F, et al. Next generation sequencing-based molecular diagnosis of retinitis pigmentosa: identification of a novel genotype-phenotype correlation and clinical refinements. *Hum Genet.* 2014; 133:331–345. [PubMed: 24154662]
111. Carter-Dawson LD, LaVail MM. Rods and cones in the mouse retina. I. Structural analysis using light and electron microscopy. *J Comp Neurol.* 1979; 188:245–262. [PubMed: 500858]

112. Jeon CJ, Strettoi E, Masland RH. The major cell populations of the mouse retina. *J Neurosci*. 1998; 18:8936–8946. [PubMed: 9786999]
113. Kovács AD, Pearce DA. Finding the most appropriate mouse model of juvenile CLN3 (Batten) disease for therapeutic studies: the importance of genetic background and gender. *Disease models & mechanisms*. 2015; 8:351–361. [PubMed: 26035843]
114. Lojewski X, et al. Human iPSC models of neuronal ceroid lipofuscinosis capture distinct effects of TPP1 and CLN3 mutations on the endocytic pathway. *Hum Mol Genet*. 2014; 23:2005–2022. [PubMed: 24271013]
115. Bell CJ, et al. Carrier testing for severe childhood recessive diseases by next-generation sequencing. *Science translational medicine*. 2011; 3:65ra64.
116. Sondhi D, et al. Partial correction of the CNS lysosomal storage defect in a mouse model of juvenile neuronal ceroid lipofuscinosis by neonatal CNS administration of an adeno-associated virus serotype rh.10 vector expressing the human CLN3 gene. *Hum Gene Ther*. 2014; 25:223–239. [PubMed: 24372003]
117. Crystal RG. Phase I. Direct CNS administration of a replication deficient adeno-associated virus gene transfer vector serotype rh.10 expressing the human CLN2 cDNA to children with late infantile neuronal ceroid lipofuscinosis (LINCL) (NCT01161576).
118. Augustine EF. Phase II. Randomized, placebo controlled trial of the safety and tolerability of mycophenolate in children with Juvenile Neuronal Ceroid Lipofuscinosis (NCT01399047).
119. Orchard P. Phase II/III. Treatment of lysosomal and peroxisomal inborn errors of metabolism by bone marrow transplantation (NCT00176904).
120. Seehafer SS, et al. Immunosuppression alters disease severity in juvenile Batten disease mice. *J Neuroimmunol*. 2011; 230:169–172. [PubMed: 20937531]

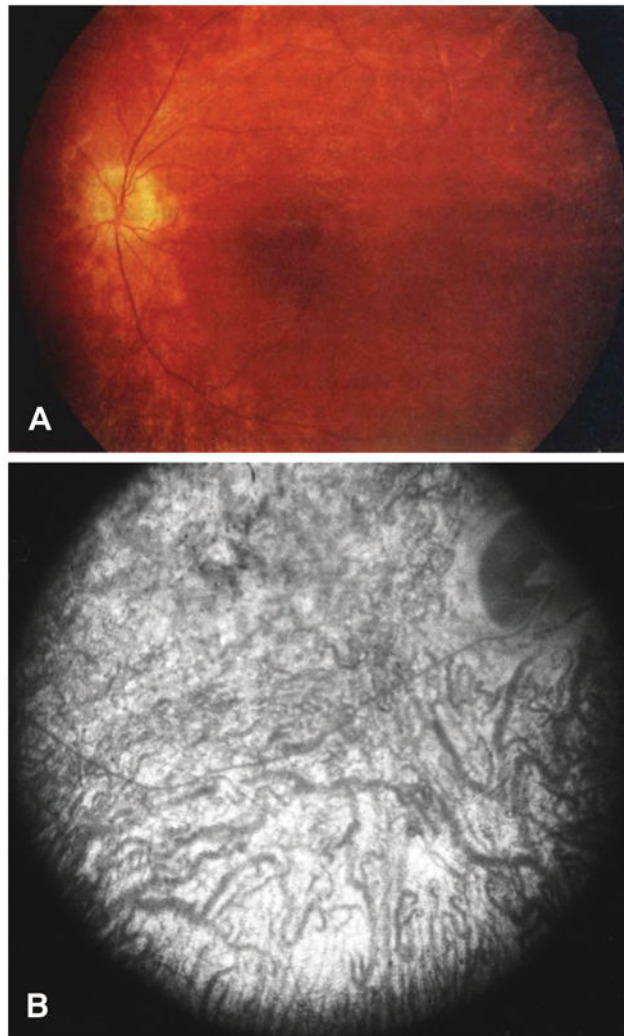


Figure 1. Fundoscopy of JNCL patient eyes. (A) Posterior pole of the left eye of an 8-year-old female JNCL patient with the common 1 kb deletion showing bull's eye maculopathy, attenuated vessels, and pale optic discs. Reproduced, with permission, from Ref. 50. (B) Angiogram with diffuse stippled hyperfluorescence in the eye of a 9-year-old JNCL patient. Reproduced, with permission, from Ref. 47.

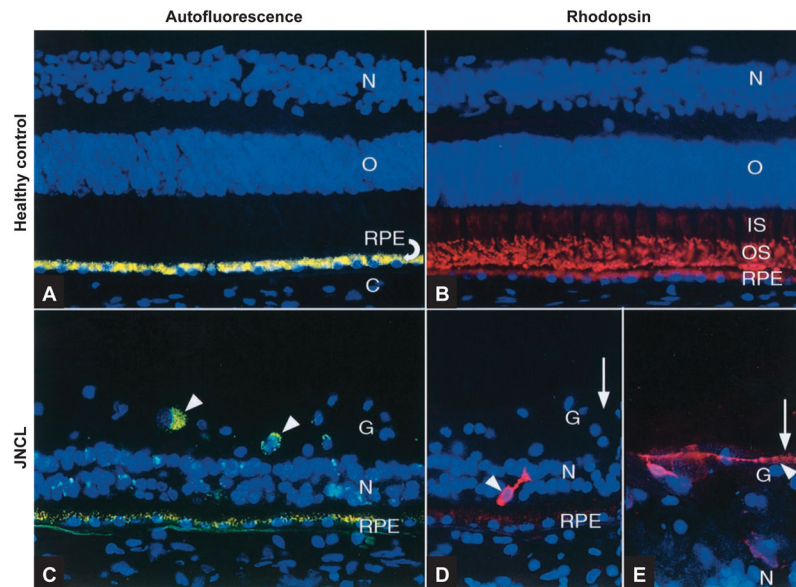


Figure 2. Fluorescence microscopy of far peripheral retina with 4',6'-diamidino-2-phenylindole (DAPI)-stained nuclei (in blue) showing reduced RPE autofluorescence and retinal degeneration in JNCL. (A) Healthy control and (C) JNCL retinal sections treated with no primary antibody. Yellow: autofluorescent lipofuscin granules; arrowheads: ganglion cells. (B) Healthy control and (D&E) JNCL retinal sections labeled with anti-rhodopsin (in red). Arrowheads: retained rhodopsin⁺ rods; the one in (E) has a long, beaded neurite. Reproduced, with permission, from Ref. 54. Abbreviations: C, choroid; RPE, retinal pigment epithelium; O, outer nuclear layer; N, inner nuclear layer; IS, rod inner segments; OS, rod outer segments; G, ganglion cell layer.

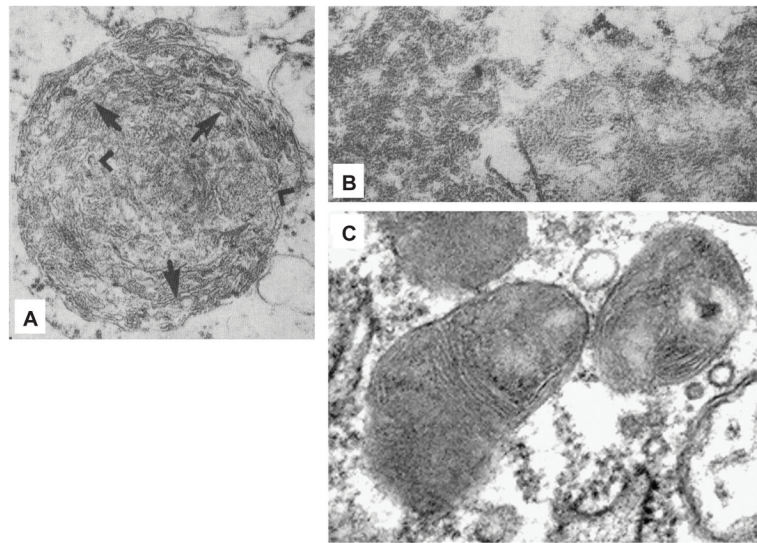


Figure 3.

Electron micrographs of retinal ganglion cells containing inclusions with (A) curvilinear and (B&C) fingerprint features. (A) An inclusion found in a JNCL patient ganglion cell with trilaminar membranes (arrows), some of them arranged in a curvilinear fashion (arrowheads) surrounded by a trilaminar unit membrane ($\times 31,000$). (B) A rare fingerprint body found in the cytoplasm of a JNCL patient ganglion cell ($\times 51,000$). A and B are reproduced, with permission, from Ref. 48. (C) Perinuclear inclusions with fingerprint profiles are abundant in the cytoplasm of a retinal ganglion cell from a 10-month-old *Cln3*^{ex7/8} homozygous mouse. Reproduced, with permission, from Ref. 77.

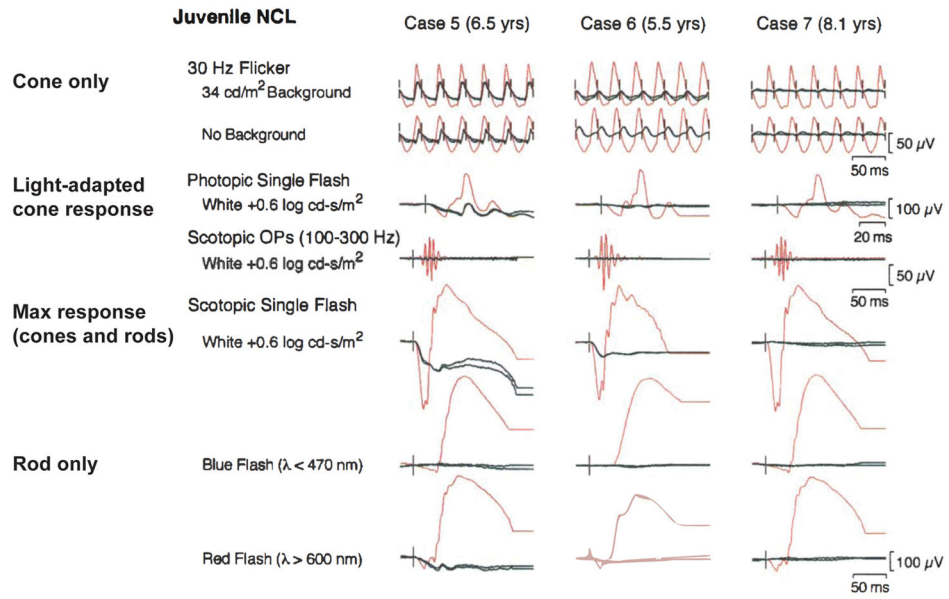


Figure 4. ISCEV standard ERGs of three JNCL patients. The tracings from each patient’s right and left eyes are shown in black. The tracings in red are for normal subjects of the same age range. Reproduced, with permission, from Ref. 50.